Formation of Heterobimetallic Zirconium/Cobalt Diimido Complexes via a Four-Electron Transformation

Bing Wu,[†] Raúl Hernández Sánchez,[‡] Mark W. Bezpalko,[†] Bruce M. Foxman,[†] and Christine M. Thomas*,[†]

[†]Department of Chemistry, Brandeis University, 415 South Street, MS 015, Waltham, Massachusetts 02454, United States

[‡]Department of Chemistry and Chemical Biology, Harvard University, 12 Oxford Street, Cambridge, Massachusetts 02139, United States

Ⓢ *Supporting Information*

ABSTRACT: The reactivity of the reduced heterobimetallic complex $Zr(^iPrNP^iPr_2)_3CoN_2$ (**1**) toward aryl azides was examined, revealing a four-electron redox transformation to afford unusual heterobimetallic zirconium/cobalt diimido complexes. In the case of *p*-tolyl azide, the diamagnetic C_3-symmetric bis(terminal imido) complex **3** is formed, but mesityl azide instead leads to asymmetric complex **4** featuring a bridging imido fragment.

Late-transition-metal coordination complexes featuring metal−ligand multiple bonds have attracted much attention because of their ability to mediate atom- or group-transfer reactions.[1] Organic azides react with transition-metal complexes to form intermediate metal azide adducts, which extrude dinitrogen to generate metal imido/nitrene compounds as the key reactive intermediates. Despite their intermediacy in a wide array of catalytic chemical transformations,[2] isolated first-row late-transition-metal imido complexes remain rare as a result of the absence of empty d orbitals to accept π donation from the imido fragment.[3] Among the few reported terminal cobalt imido species,[4−11] only two examples of thermally accessible open-shell configurations have been reported: Theopold's (Tp*)-Co(III)(NAd) [Tp* = hydrotris(3-*tert*-butyl-5-methylpyrazolyl)-borate; Ad = adamantyl] complex undergoes a spin transition to a thermally accessible open-shell state,[8,12,13] and Betley's cobalt imido complex (^{Ar}L)Co(III)(N*t*Bu) [^{Ar}L = 5-mesityl-1,9-(2,4,6-triphenylphenyl)dipyrromethene] undergoes a thermally induced spin transition from an $S = 0$ to an $S = 2$ state.[11] Tris(phosphine)-ligated cobalt imido species, on the other hand, typically adopt a low-spin $S = 0$ configuration.[4,5]

Our group has been investigating both homo- and heterobimetallic complexes featuring first-row transition metals supported by C_3-symmetric tris(phosphinoamide) ligand frameworks in an effort to better understand metal−metal bonding and to explore the possibility of promoting reactivity via metal−metal cooperativity.[14] In this context, our group has previously demonstrated that the reduced heterobimetallic complex (THF)Zr(MesNP^{i}Pr$_2$)$_3$CoN$_2$ (THF = tetrahydrofuran; Mes = 2,4,6-trimethylphenyl) undergoes both one- and two-electron oxidation during the activation of C−X,[15] E−H (E = N, S, O),[16,17] and C═O bonds.[18,19] A recent XANES Co and Zr K-edge study has shown that the reduced heterobimetallic complexes are best described as zwitterionic Zr(IV)Co(−I) species,

suggesting that the one- and two-electron redox processes are cobalt-centered.[20] In the context of metal−ligand multiple bonds, it was found that the C═O bond of benzophenone oxidatively adds across the Zr−Co bond of (THF)Zr-(MesNP^{i}Pr$_2$)$_3$CoN$_2$ in a stepwise fashion, generating a μ-oxo and an unusual Co═CPh$_2$ fragment.[18] Therefore, we hypothesized that a similar heterobimetallic framework may stabilize a cobalt imido species. Herein, we report heterobimetallic diimido complexes prepared via the addition of organic azides to a similar highly reduced, coordinatively unsaturated heterobimetallic zirconium/cobalt complex, an overall four-electron process.

The addition of 1 equiv of ^{t}BuN$_3$ to Zr(^{i}PrNP^{i}Pr$_2$)$_3$CoN$_2$ (**1**)[21] did not lead to dinitrogen extrusion or imide formation but instead cleanly produced the two-electron-oxidized $S = 1$ azide adduct (η^2-^{i}PrNP^{i}Pr$_2$)Zr(μ_2-$\eta^1\eta^3$-^{t}BuN$_3$)(^{i}PrNP^{i}Pr$_2$)$_2$Co (**2**; see the Supporting Information, SI). Consistent with other reports of enhanced reactivity of aryl azides compared to alkyl azides,[22,23] aryl azides were shown to extrude dinitrogen quite readily upon addition to **1** to form stable imido products. The treatment of **1** with 2 equiv of (*p*-tolyl)N$_3$ rapidly leads to dinitrogen evolution and clean formation of diamagnetic green (*p*-tolyl)N═Zr-(^{i}PrNP^{i}Pr$_2$)$_3$Co═N(*p*-tolyl) (**3**; Scheme 1). Complex **3** is characterized by one ^{31}P NMR signal at 51.0 ppm, indicating a C_3-symmetric structure. Single-crystal X-ray diffraction reveals
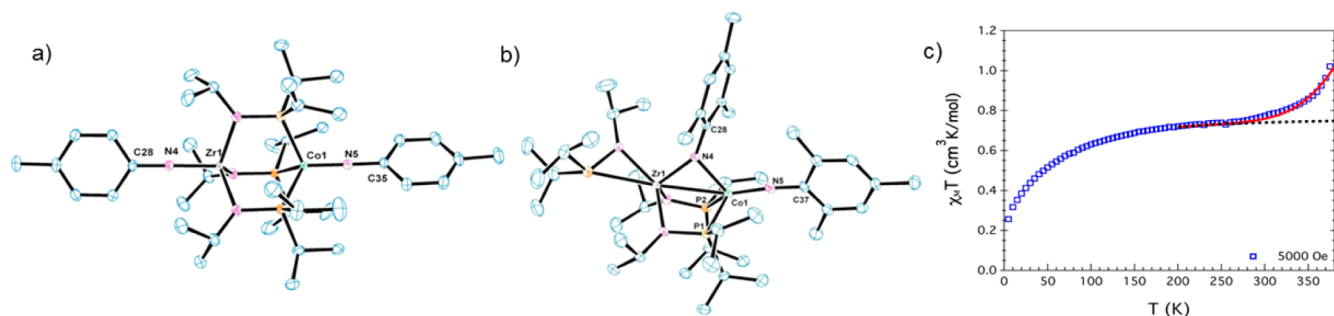
Scheme 1
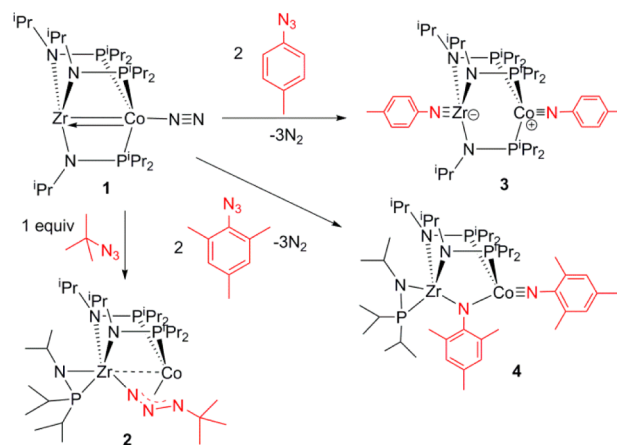
Figure 1. (a and b) Displacement ellipsoid (50%) representations of **3** (a) and **4** (b). All hydrogen atoms have been omitted for clarity, and only one position of the disordered isopropyl groups is shown for **3**. (c) Variable-temperature magnetic susceptibility for **4** under a dc applied field of 0.5 kOe (open blue squares). The black dotted line represents the simulation of 25.5% of the molecules trapped in the $S = 2$ state. The red trace corresponds to the best simulation of the spin crossover with $\Delta H = 2650$ cm^{-1} and $T_c = 475$ K.

that an unusual four-electron process has occurred to form the zwitterionic zirconium(IV)−cobalt(III) complex **3** featuring terminal imido fragments bound to both cobalt and zirconium (Figure 1a). Several low-coordinate terminal cobalt imido complexes have been reported in recent years,[6−11] including those with a pseudotetrahedral tris(phosphine) coordination environment.[4,5] The Co−N bond distance [1.6701(18) Å] and the Co−N−C angle [178.45(16)°] in **3** compare well with other cobalt imido complexes, in support of the metal−ligand triple bond expected based on symmetry considerations. Terminal zirconium imides are much more common, and the Zr−N bond distance [1.8893(17) Å] is within the range observed among these known compounds. The elongated Zr−Co interatomic distance of 3.1734(3) Å indicates no interaction between the two metal centers in **3**. Notably, preliminary results suggest that a similar diimido complex is formed when complex **1** is treated with azobenzene.

The addition of 2 equiv of MesN$_3$ to a THF solution of **1** also results in the rapid evolution of dinitrogen accompanied by a color change. However, in this case, the product **4** is dark brown. In contrast to complex **3**, the ^{1}H NMR spectrum of **4** features both broad paramagnetically shifted resonances and more well-defined resonances in the typical 0−10 ppm diamagnetic region (Figures S4 and S5 in the SI). Furthermore, no ^{31}P{^{1}H} NMR signal is observed for complex **4** at room temperature. The solid-state structure of **4** obtained using X-ray crystallography reveals a zirconium(IV)−cobalt(III) diimido complex, but in this case, an asymmetric structure is adopted with one terminal cobalt imide and a second imide bridging zirconium and cobalt, (η^2-^{i}PrNP^{i}Pr$_2$)Zr(μ-NMes)(^{i}PrNP^{i}Pr$_2$)$_2$Co≡NMes (**4**; Figure 1b). The Co−N bond distance of 1.6827(16) Å is slightly longer than that of **3**, and the Co−N−C angle of 169.66(14)° is slightly bent, but these parameters remain consistent with a triple-bonded cobalt imido fragment. The metal−N4 distances associated with the bridging imido ligand are substantially elongated in comparison to the terminal imido ligands in **3** and **4**, particularly the Co−N4 distance [2.0123(15) Å].

As mentioned above, the ^{1}H NMR spectrum of bridged diimido complex **4** contains small paramagnetic features. Repeated solution magnetic moment measurements on analytically pure samples of **4** in C$_6$D$_6$ at room temperature provided a magnetic moment of $\mu_{eff} = 1.96$ μ_B, a value inconsistent with a compound that should have an even number of electrons. No ν(N−H) stretches were observed in the solid-state IR spectrum of **4**, and no one-electron peaks were observed in the difference Fourier map of crystals of **4**, excluding any possibility that the imide ligands identified in the solid-state structure of **4** were

actually protonated amides. Thus, the spectroscopic behavior and solution magnetic susceptibility of complex **4** suggest a mixture of high- and low-spin compounds in solution at room temperature. Cooling an NMR sample of **4** in toluene-d_8 resulted in the broadening and downfield shifting of the ^{1}H resonances in the 10−75 ppm range at −50 °C (Figure S6 in the SI) and the appearance of two ^{31}P{^{1}H} NMR signals at 56 and 5 ppm, consistent with cobalt- and zirconium-bound phosphines, respectively. The Curie behavior of the paramagnetically shifted resonances (Figure S9 in the SI) and the absence of changes to the resonances in the diamagnetic region of the ^{1}H NMR of **4** suggest that interconversion of the two spin states is slower than the NMR time scale at low temperature.[24] As the temperature of a solution of **4** was increased from room temperature to 60 °C, the downfield signals in the ^{1}H NMR shifted upfield but also broadened considerably (Figure S7 in the SI). Measurement of the magnetic susceptibility of complex **4** in solution using Evans' method over the −50 to +60 °C temperature range revealed a modest but consistent increase in the magnetic susceptibility as a function of the temperature. Indeed, recent examples have shown that spin transitions are often sharper in the solid state than in solution.[25−27]

To better understand the unique magnetic behavior of complex **4**, variable-temperature direct-current (dc) magnetic susceptibility data were collected from 5 to 375 K (Figure 1c). The plot of $\chi_M T$ versus T displays a sharp increase at high temperature, reaching 1.02 cm^{3}K/mol at 375 K. As the temperature decreases, the susceptibility data reach constant values of around 0.65−0.70 cm^{3}K/mol in the temperature range from 100 to 250 K. They decrease further to 0.26 cm^{3}K/mol at 5 K. As the data indicate, a singlet ground state was never achieved. It is our hypothesis that some fraction of the higher-spin-state molecules remain trapped at low temperature, as observed by others.[11,28,29] To gain further insight into the electronic nature of the trapped state, we collected variable-temperature, variable-field magnetization data over the temperature range of 1.8−10 K and at fields of 1−7 T (Figure S17 in the SI). The resulting reduced magnetization plot showed a sequence of non-superimposable isofield curves. Saturation occurred at $M = 0.59$ μ_B at 1.8 K and 7 T, thus much lower than expected for an $S = 1$ or $S = 2$ spin state. The $\chi_M T$ data were simulated as a spin transition (ΔH and T_c) by using eq S.1 in the SI, in which c_S is the fraction of molecules trapped in the higher spin state at low T.[11,27,28] Two scenarios were considered: (1) a singlet-to-triplet spin crossover; (2) a singlet-to-quintet spin crossover. The simulation parameters for the former case showed clearly that a triplet state was not at play (Figure S16a in the SI). A model that

satisfactorily fits the reduced magnetization (Figure S17 in the SI) and the $\chi_M T$ data (Figure 1c) was obtained by considering a singlet-to-quintet spin crossover where 25.5% of the molecules are trapped in the high-spin state at low temperature. This appears to be both a solution and a solid-state phenomenon.[30]

In summary, a reduced heterobimetallic zirconium/cobalt complex reacts readily with organic azides. Aryl azides react via a four-electron cobalt-centered redox process to generate zirconium(IV)−cobalt(III) diimido species. A terminal cobalt-(III) imido fragment is afforded in all cases, but depending on the aryl substituents, either a C_3-symmetric bis(terminal imido) complex or an asymmetric imido-bridged complex is formed. The compound featuring a zirconium/cobalt bridging imide and cobalt terminal imide shows unusual magnetic behavior and appears to undergo a spin transition from $S = 0$ to $S = 2$ near room temperature. Further studies on this magnetic phenomenon and its variability with imido substituents and studies on the reactivity of these heterobimetallic imido complexes are ongoing.

■ ASSOCIATED CONTENT

Ⓢ Supporting Information

Experimental procedures and additional spectroscopic, crystallographic, and magnetic susceptibility data for **2**−**4**, including a CIF file. This material is available free of charge via the Internet at http://pubs.acs.org.

■ AUTHOR INFORMATION

Corresponding Author
*E-mail: thomasc@brandeis.edu.

Notes
The authors declare no competing financial interest.

■ ACKNOWLEDGMENTS

■ REFERENCES

(1) (a) Nugent, W. A.; Mayer, J. M. *Metal−Ligand Multiple Bonds*; Wiley: New York, 1998. (b) Wigley, D. E. Organoimido Complexes of the Transition Metals. In *Progress in Inorganic Chemistry*; John Wiley & Sons, Inc.: New York, 2007; pp 239−482. (c) Man, W.-L.; Lam, W. W. Y.; Lau, T.-C. *Acc. Chem. Res.* **2014**, *47*, 427−439. (d) Woo, L. K. *Chem. Rev.* **1993**, *93*, 1125−1136. (e) Du Bois, J.; Tomooka, C. S.; Hong, J.; Carreira, E. M. *Acc. Chem. Res.* **1997**, *30*, 364−372. (f) Eikey, R. A.; Abu-Omar, M. M. *Coord. Chem. Rev.* **2003**, *243*, 83−124. (g) Saouma, C. T.; Peters, J. C. *Coord. Chem. Rev.* **2011**, *255*, 920−937. (h) Che, C.-M.; Lo, V. K.-Y.; Zhou, C.-Y.; Huang, J.-S. *Chem. Soc. Rev.* **2011**, *40*, 1950−1975.

(2) (a) Fantauzzi, S.; Gallo, E.; Caselli, A.; Ragaini, F.; Casati, N.; Macchi, P.; Cenini, S. *Chem. Commun.* **2009**, 3952−3954. (b) Liu, Y.; Wei, J.; Che, C.-M. *Chem. Commun.* **2010**, *46*, 6926−6928. (c) Lyaskovskyy, V.; Suarez, A. I. O.; Lu, H.; Jiang, H.; Zhang, X. P.; de Bruin, B. *J. Am. Chem. Soc.* **2011**, *133*, 12264−12273. (d) King, E. R.; Hennessy, E. T.; Betley, T. A. *J. Am. Chem. Soc.* **2011**, *133*, 4917−4923. (e) Hennessy, E. T.; Betley, T. A. *Science* **2013**, *340*, 591−595.

(3) Winkler, J.; Gray, H. Electronic Structures of Oxo−Metal Ions. In *Molecular Electronic Structures of Transition Metal Complexes I*; Mingos, D. M. P., Day, P., Dahl, J. P., Eds.; Springer: Berlin, 2012; Vol. *142*, pp 17−28.

(4) Jenkins, D. M.; Betley, T. A.; Peters, J. C. *J. Am. Chem. Soc.* **2002**, *124*, 11238−11239.

(5) Betley, T. A.; Peters, J. C. *J. Am. Chem. Soc.* **2003**, *125*, 10782−10783.

(6) Hu, X.; Meyer, K. *J. Am. Chem. Soc.* **2004**, *126*, 16322−16323.

(7) Dai, X.; Kapoor, P.; Warren, T. H. *J. Am. Chem. Soc.* **2004**, *126*, 4798−4799.

(8) Shay, D. T.; Yap, G. P. A.; Zakharov, L. N.; Rheingold, A. L.; Theopold, K. H. *Angew. Chem., Int. Ed.* **2005**, *44*, 1508−1510.

(9) Cowley, R. E.; Bontchev, R. P.; Sorrell, J.; Sarracino, O.; Feng, Y.; Wang, H.; Smith, J. M. *J. Am. Chem. Soc.* **2007**, *129*, 2424−2425.

(10) Jones, C.; Schulten, C.; Rose, R. P.; Stasch, A.; Aldridge, S.; Woodul, W. D.; Murray, K. S.; Moubaraki, B.; Brynda, M.; La Macchia, G.; Gagliardi, L. *Angew. Chem., Int. Ed.* **2009**, *48*, 7406−7410.

(11) King, E. R.; Sazama, G. T.; Betley, T. A. *J. Am. Chem. Soc.* **2012**, *134*, 17858−17861.

(12) Wasbotten, I. H.; Ghosh, A. *Inorg. Chem.* **2007**, *46*, 7890−7898.

(13) Shay, D. T.; Yap, G. P. A.; Zakharov, L. N.; Rheingold, A. L.; Theopold, K. H. *Angew. Chem., Int. Ed.* **2006**, *45*, 7870−7870.

(14) Krogman, J. P.; Thomas, C. M. *Chem. Commun.* **2014**, *50*, 5115−5127.

(15) Thomas, C. M.; Napoline, J. W.; Rowe, G. T.; Foxman, B. M. *Chem. Commun.* **2010**, *46*, 5790−5792.

(16) Napoline, J. W.; Bezpalko, M. W.; Foxman, B. M.; Thomas, C. M. *Chem. Commun.* **2013**, *49*, 4388−4390.

(17) Napoline, J. W.; Krogman, J. P.; Shi, R.; Kuppuswamy, S.; Bezpalko, M. W.; Foxman, B. M.; Thomas, C. M. *Eur. J. Inorg. Chem.* **2013**, *2013*, 3874−3882.

(18) Marquard, S. L.; Bezpalko, M. W.; Foxman, B. M.; Thomas, C. M. *J. Am. Chem. Soc.* **2013**, *135*, 6018−6021.

(19) Krogman, J. P.; Foxman, B. M.; Thomas, C. M. *J. Am. Chem. Soc.* **2011**, *133*, 14582−14585.

(20) Krogman, J. P.; Gallagher, J. R.; Zhang, G.; Hock, A. S.; Miller, J. T.; Thomas, C. M. *Dalton Trans.* **2014**, *43*, 13852−13857.

(21) Greenwood, B. P.; Rowe, G. T.; Chen, C.-H.; Foxman, B. M.; Thomas, C. M. *J. Am. Chem. Soc.* **2010**, *132*, 44−45.

(22) Mankad, N. P.; Müller, P.; Peters, J. C. *J. Am. Chem. Soc.* **2010**, *132*, 4083−4085.

(23) Intrieri, D.; Zardi, P.; Caselli, A.; Gallo, E. *Chem. Commun.* **2014**, *50*, 11440−11453.

(24) We note that spin crossover is usually much faster than the NMR time scale, so the behavior reported here is unusual. While we can envision several possible explanations for this phenomenon, including scenarios involving additional equilibria in solution, more extensive further studies will be needed to fully understand this behavior.

(25) Weber, B.; Walker, F. A. *Inorg. Chem.* **2007**, *46*, 6794−6803.

(26) Jeon, I.-R.; Park, J. G.; Haney, C. R.; Harris, T. D. *Chem. Sci.* **2014**, *5*, 2461−2465.

(27) Khan, O. *Molecular Magnetism*; VCH: New York, 1993.

(28) Scepaniak, J. J.; Harris, T. D.; Vogel, C. S.; Sutter, J.; Meyer, K.; Smith, J. M. *J. Am. Chem. Soc.* **2011**, *133*, 3824−3827.

(29) Bowman, A. C.; Milsmann, C.; Bill, E.; Turner, Z. R.; Lobkovsky, E.; DeBeer, S.; Wieghardt, K.; Chirik, P. J. *J. Am. Chem. Soc.* **2011**, *133*, 17353−17369.

(30) To discount the explanation that the unusual magnetic behavior observed for complex **4** was the result of an unrelated paramagnetic impurity, the following important experiments were conducted: (1) Solid-state magnetometry data were collected for a few different batches of crystalline complex **4**. In all cases, similar variable-temperature magnetic behavior was observed. (2) Solution magnetic moment data were collected using Evans' method on several different samples of complex **4** at room temperature, and a similar magnetic moment was obtained for all samples. (3) Visual inspection of crystalline samples of complex **4** under a microscope revealed just one type of crystalline morphology, and a unit cell determination of several different crystals revealed identical unit cells. (4) A crystalline sample of **4** was investigated using powder X-ray diffraction, revealing a phase-pure material (see the SI).